Volume 53
Number 1
7 January 2024
Pages 1-366

Dalton Transactions

An international journal of inorganic chemistry

rsc.li/dalton

ISSN 1477-9226

ROYAL SOCIETY OF CHEMISTRY

PAPER

Artur Kasprzak *et al.*

Oxidation-derived anticancer potential of sumanene–ferrocene conjugates

Dalton Transactions

ROYAL SOCIETY OF CHEMISTRY

PAPER

View Article Online
View Journal | View Issue

Check for updates

Cite this: *Dalton Trans.*, 2024, **53**, 56

Oxidation-derived anticancer potential of sumanene–ferrocene conjugates†

Artur Kasprzak, *[a] Agnieszka Zuchowska, [a] Pawel Romanczuk, [a] Agata Kowalczyk, [b] Ireneusz P. Grudzinski, [c] Anna Malkowska, [c] Anna M. Nowicka [b] and Hidehiro Sakurai [d,e]

An effective synthetic protocol towards the oxidation of sumanene–ferrocene conjugates bearing one to four ferrocene moieties has been established. The oxidation protocol was based on the transformation of Fe^{II} from ferrocene to Fe^{III}-containing ferrocenium cations by means of the treatment of the title organometallic buckybowls with a mild oxidant. Successful isolation of these ferrocenium-tethered sumanene derivatives **5–7** gave rise to the biological evaluation of the first, buckybowl-based anticancer agents, as elucidated by *in vitro* assays with human breast adenocarcinoma cells (MDA-MB-231) and embryotoxicity trials in zebrafish embryos supported with *in silico* toxicology studies. The designed ferrocenium-tethered sumanene derivatives featured attractive properties in terms of their use in cancer treatments in humans. The tetra-ferrocenium sumanene derivative **7** featured especially beneficial biological features, elucidated by low (<40% for 10 μM) viabilities of MDA-MB-231 cancer cells together with a 1.4–1.7-fold higher viability of normal cells (human mammary fibroblasts, HMF) for respective concentrations. Compound **7** featured significant cytotoxicity against cancer cells thanks to the presence of sumanene and ferrocenium moieties; the latter motif also provided the selectivity of anticancer action. The biological properties of **7** were also improved in comparison with those of native building blocks, which suggested the effects of the presence of the sumanene skeleton towards the anticancer action of this molecule. Ferrocenium-tethered sumanene derivatives exhibited potential towards the generation of reactive oxygen species (ROS), responsible for biological damage to the cancer cells, with the most efficient generation of the tetra-ferrocenium sumanene derivative **7**. Derivative **7** also did not show any embryotoxicity in zebrafish embryos at the tested concentrations, which supports its potential as an effective and cancer-specific anticancer agent. *In silico* computational analysis also showed no chromosomal aberrations and no mutation with AMES tests for the compound **7** tested with and without microsomal rat liver fractions, which supports its further use as a potent drug candidate in detailed anticancer studies.

Received 14th November 2023,
Accepted 28th November 2023

DOI: 10.1039/d3dt03810f

rsc.li/dalton

Open Access Article. Published on 30 November 2023. Downloaded on 2/9/2026 12:15:48 PM.
This article is licensed under a Creative Commons Attribution 3.0 Unported Licence.

Introduction

Sumanene (**1**; see Fig. 1a) is a bowl-shaped buckybowl compound that was first synthesized in 2003.[1] The possibilities of (i) functionalization of sumanene at the benzylic and aromatic positions,[2–5] as well as (ii) the generation of sumanenyl carbanions[6,7] were demonstrated. As the result, various organometallic complexes comprising sumanene were synthesized, and these derivatives can be grouped into two general classes. The first class of compounds employed sumanene itself as a ligand, with organometallic complexes containing ruthenium,[8,9] iron,[9–11] or zirconium[12] as representative examples. The second class of organometallic complexes comprising sumanene are the derivatives in which the structural moiety attached to the sumanene skeleton plays a role of a ligand. This approach for molecule design was recently employed for the synthesis of ruthenium complexes containing sumanene molecules functionalized with a pincer ligand[13] or sumanene-containing organic capsules.[14] Ferrocene (Fc)-containing sumanene derivatives can be regarded as an interesting class of sumanene organometallic congeners, not only

[a]*Faculty of Chemistry, Warsaw University of Technology, Noakowskiego Str. 3, 00-664 Warsaw, Poland. E-mail: artur.kasprzak@pw.edu.pl*
[b]*Faculty of Chemistry, University of Warsaw, Pasteura Str. 1, 02-093 Warsaw, Poland*
[c]*Faculty of Pharmacy, Medical University of Warsaw, Banacha Str. 1, 02-097 Warsaw, Poland*
[d]*Division of Applied Chemistry, Graduate School of Engineering, Osaka University, 2-1 Yamadaoka, Suita, 565-0871 Osaka, Japan*
[e]*Innovative Catalysis Science Division, Institute for Open and Transdisciplinary Research Initiatives (ICS-OTRI), Osaka University, Suita, Osaka 565-0871, Japan*

†Electronic supplementary information (ESI) available: Materials and methods, experimental section, compound characterization data, spectrofluorimetric and voltammetric data on the molecular receptor application, and details on biological assays. See DOI: https://doi.org/10.1039/d3dt03810f

This journal is © The Royal Society of Chemistry 2024

Open Access Article. Published on 30 November 2023. Downloaded on 2/9/2026 12:15:48 PM.
This article is licensed under a Creative Commons Attribution 3.0 Unported Licence.

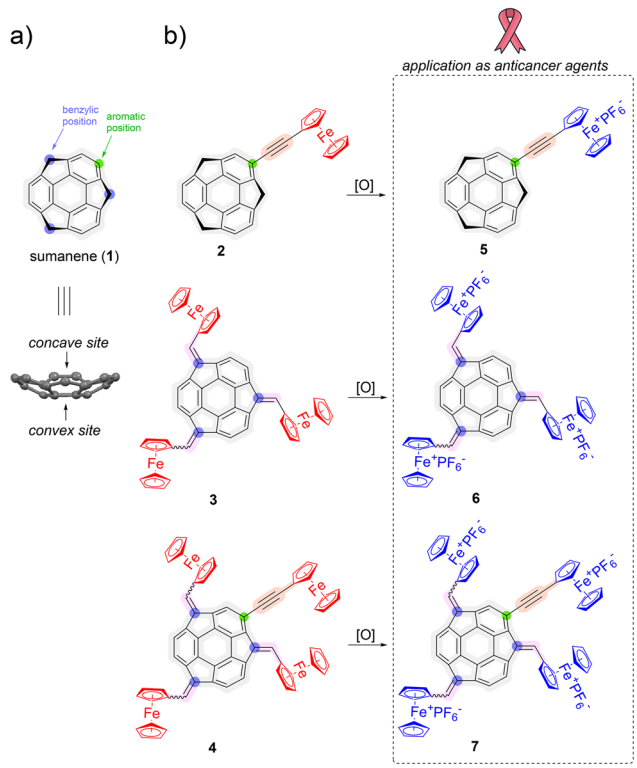

Fig. 1 (a) Structure of sumanene (**1**); (b) sumanene derivatives **2–7** investigated herein, together with the graphical representation of the aims of this work.

in the field of structural chemistry buckybowls, but also towards their applied sciences. For example, recent studies revealed that such conjugates can be applied in cesium cation selective voltammetric sensors.[15–18]

Fc-tethered compounds have been widely explored over the years in different areas of applications. This is because Fc is an air-stable and easy to modify molecule with various prospective applications.[19–21] Cancer research is one of the most important applications of Fc containing systems.[19,20,22–25] Interestingly, the derivatives comprising ferrocenium cations (Fc^+) were reported to be attractive and effective anticancer agents. First reports are dated back to 1984, when Köpf-Maier and co-workers reported the anticancer action of Fc^+ salts.[26] While Fc did not feature significant toxicity towards cancer cells, Fc^+ inhibited cancer cell growth, which was further supported by other studies.[27,28] Detailed studies on this topic revealed that Fc^+ features the improved properties of generating reactive oxygen species, such as $OH^{\bullet}$, which in consequence lead to the formation of radical metabolites responsible for biological damage to the cells, *e.g.*, oxidative DNA damage.[27–30] Despite these beneficial biological properties of Fc^+ containing systems, the reports on their use in cancer treatments are limited, mostly because of difficulties in the synthesis of such a class of compounds.

Due to the origin of buckybowls from carbon allotropes, whose use in cancer nanotechnology has been widely studied over the years,[31–33] prospective biological applications of buckybowls can be considered. However, to the best of our knowledge, the reported studies on applications of buckybowls in medicinal chemistry are extremely sparse. The reports only include corannulene derivatives as cholera toxin inhibitors[34] and click chemistry derived corannulene glycoconjugates as cancer-specific molecules.[35] The potential biological behaviors of sumanene derivatives only include recent (2021–2023) theoretical studies[36,37] on the prospective use of sumanene molecules in drug delivery. Interestingly, in these computational works, the bowl-to-bowl inversion property of sumanene molecules was considered as the driving force towards the design of effective drug delivery systems. Therefore, inspired by the promising anticancer effects of Fc^+-tethered compounds as well as highly limited reports on the biological applications of functionalized buckybowls, herein, in pursuit of gaining new knowledge on the synthesis, properties and applications of sumanene derivatives, we report for the first time the synthesis and the assessment of the anticancer potential of sumanene-derivatives **5–7** bearing various numbers of Fc^+ units (from one to four, see Fig. 1b). Fe^{III}-containing derivatives **5–7** were obtained *via* the treatment of ferrocene (Fe^{II}) containing compounds **2–4** with a mild oxidant. Considering that the most common cancer worldwide is breast cancer,[38,39] cytotoxicity profiles were estimated *in vitro* against human breast adenocarcinoma cells (MDA-MB-231) and human mammary fibroblasts (HMF) as normal cells. As a result of this work, a promising class of metallocene-tethered buckybowl-based anticancer agents was established.

Results and discussion

Synthesis and characterization of sumanene–ferrocene conjugates 2–4

A Materials and methods section, as well as full experimental details, can be found in ESI, Subsection S1.2† (synthetic procedures are also listed below in the Experimental section). 2-(Ferrocenylethynyl)sumanene (**2**)[17] and tris(ferrocenylmethidene)sumanene (**3**)[16] (Fig. 1b) were synthesized according to the literature protocols. The synthesis of the tetraferrocenylated sumanene derivative **4** (Fig. 2) was based on the condensation-type reaction[16] and employed formylferrocene (**8**) and compound **2**[17] as the starting materials. Notably, the reported procedures for the syntheses of tris-substituted sumanene

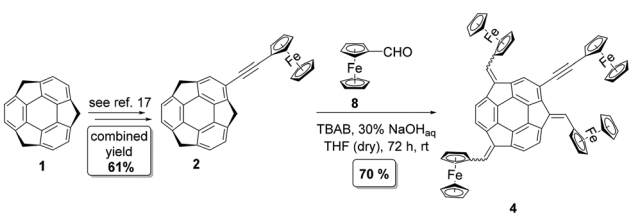

Fig. 2 Synthesis of the sumanene derivative tetrasubstituted with ferrocene (**4**).

Open Access Article. Published on 30 November 2023. Downloaded on 2/9/2026 12:15:48 PM.
This article is licensed under a Creative Commons Attribution 3.0 Unported Licence.

derivatives employing the condensation-type reaction[16,18,40–42] to date only employed native sumanene as the starting material. Our successful experiment with **4** demonstrated that it is possible to subject a sumanene derivative functionalized at the aromatic carbon to this process. The formation of compound **4** was confirmed by NMR spectroscopy, as well as high-resolution mass spectrometry (HRMS). Copies of the NMR spectra and the respective discussion on **4** can be found in ESI, Section S2,† whilst the HRMS spectra are presented in ESI, Section S3.†

A profile of the UV-vis spectrum of **4** was different from that for the parent **2** and was similar to the respective spectrum of **3**, with the three major absorption maxima (λ_{max}) between 245 and 535 nm (the UV-Vis and emission spectra of **4** are presented in ESI, Section S4†). Emission spectroscopy studies revealed that the compound **4** is a red-light emitter (λ_{em} = 640 nm). The slightly lower emission intensity of **4** in comparison with that of **3** was ascribed to the fact that Fc is an emission (excited states) quencher.[43,44] Cyclic voltammetry experiments with **4** revealed one pair of current signals related to the reversible Fc redox process (Fig. 3). This suggested that the Fc units in **4** might not be electronically communicated. Since the intensity of the Fc electrooxidation signal varied linearly *versus* the square root of the scan rate, it can be concluded that the rate-limiting step in the electrode reaction was the diffusion of the depolarizer to the electrode surface.[45]

Taking into account that sumanene–ferrocene conjugates have been recently reported to feature caesium cation (Cs^+) selective trapping properties,[15–18] which were based on the non-covalent cation–π interactions between Cs^+ and the concave site of the sumanene bowl,[7,15,46] the prospective use of compound **4** as the Cs^+ recognition material was investigated using emission spectroscopy and voltammetry. The detailed studies on this topic are discussed in ESI, Sections S5 (spectroscopy) and S6 (electrochemistry).† In brief, despite being structurally sophisticated, the tetrasubstituted sumanene derivative **4** displayed a property of selective interaction with Cs^+. The estimated limit of detection value for the constructed voltammetric sensor (45 nM) was not as satisfactory as for the monoferrocenyl sumanenes (6–9 nM) and compound **3** (20 nM; see the comparison data in ESI, Section S6†). This trend could be ascribed to the steric factors towards trapping Cs^+ by two sumanene bowls within **4**.

Oxidation of sumanene–ferrocene conjugates 2–4 to the respective products 5–7 bearing ferrocenium cations

Voltammetric analyses revealed that compounds **2**,[17] **3**[16] and **4** are electroactive, and this electroactivity results from the presence of Fc units in these molecules. Taking into account the demonstrated redox activity of Fc-containing systems,[19,47–49] we hypothesized that it is possible to oxidize the Fc units in the structures of compounds **2–4** into the respective Fc^+, leading to the creation of buckybowls bearing Fc^+ moieties, namely compounds **5–7** (Fig. 4). The commonly used oxidants for the oxidation of Fe^{II} to Fc^{III} (oxidation of Fc to Fc^+) include, but are not limited, to nitrosonium and nitronium salts,[50] hypochlorite salts,[51] benzoquinone and its derivatives,[52–54] or iron(III) salts.[49,52,55,56]

To oxidize sumanene–Fc conjugates **2–4** to the Fc^+-containing compounds **5–7**, silver(I) hexafluorophosphate ($AgPF_6$) was selected as an easy-to-handle oxidant, and the properties of oxidizing Fc to ferrocenium hexafluorophosphate ($FcPF_6$) in dichloromethane (DCM) solutions were demonstrated.[57] The reaction scheme for synthesizing compounds **5–7** is presented in Fig. 4. Full experimental details can be found in ESI, Sections S1–S4.† In brief, the dropwise addition of a DCM solution of $AgPF_6$ at −20 °C to a solution of **2–4** resulted in a significant colour change, as well as the formation of a brownish precipitate, as visualized in Fig. 4 for compound **7**.[58] Such behaviours were reported as typical of oxidizing Fc and its

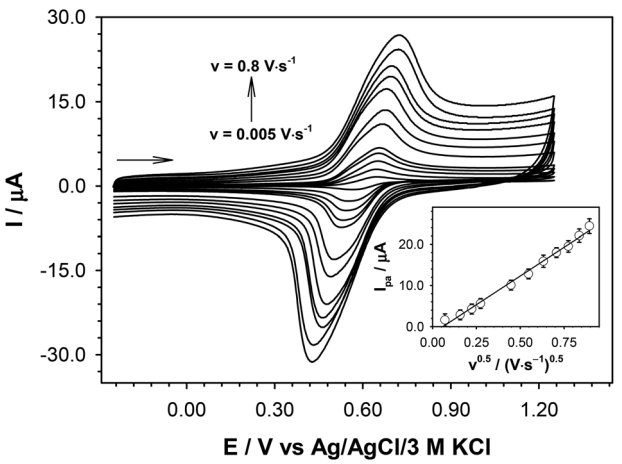

Fig. 3 Cyclic voltammograms of compound **4** recorded in DCM with the addition of tetrabutylammonium hexafluorophosphate ($TBAPF_6$). Inset: Dependencies of anodic peak current *vs.* square root of scan rate. Experimental conditions: $C_{compound}$ **4** = 0.1 mM, C_{TBAPF_6} = 50 mM, glassy carbon disk electrode (⌀ = 3 mm); T = 21 °C.

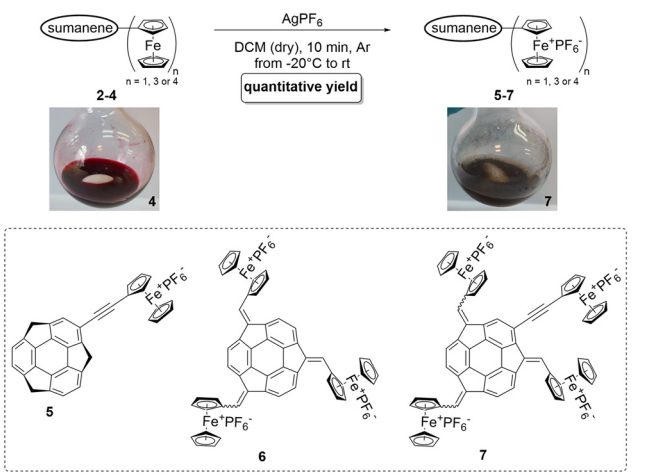

Fig. 4 Oxidation of the sumanene–ferrocene conjugates **2–4** to Fc^+-containing compounds **5–7**. Solution colours before and after the reaction in the representative synthesis of **7** from **4** are also presented.

This journal is © The Royal Society of Chemistry 2024

Open Access Article. Published on 30 November 2023. Downloaded on 2/9/2026 12:15:48 PM. This article is licensed under a Creative Commons Attribution 3.0 Unported Licence.

derivatives.[48,49,53,57,59] The syntheses of compounds **5–7** were chromatography-free, since the products were isolated by filtration and washing with ethanol (EtOH) and DCM. The reaction yields of **5–7** were quantitative. The oxidation of **2–4** to **5–7** resulted in significant changes in the solubility profiles. While Fc-containing starting materials **2–4** were well-soluble in many commonly used organic solvents, including chloroalkanes (DCM and $CHCl_3$), aromatics (PhMe and PhCl), and tetrahydrofuran (THF) and insoluble in dimethylsulfoxide (DMSO), Fc^+-containing products **5–7** were soluble in acetone and DMSO.

The formation of compounds **5–7** was confirmed by NMR spectroscopy, HRMS and elemental analysis. Copies of the NMR spectra of **5–7** and the respective discussion can be found in ESI, Section S2,† whilst the HRMS spectra of **5–7** are presented in Section S3.† In brief, the NMR spectra of **5–7** measured in deuterated acetone ($(CD_3)_2CO$) featured broad signals with chemical shift (δ_H) values higher than 15 ppm. This feature was ascribed to the presence of paramagnetic Fc^+ units in the structures of compounds **5–7**, which is consistent with the literature data for the simple Fc^+-containing molecules.[48,57,60] The signal coming from the presence of PF_6^- units in **5–7** (δ_F from −72.96 ppm to −77.70 ppm) was also clearly detected by ^{19}F NMR experiments.

The change in the oxidation state of iron (from Fe^{II} to Fe^{III}) also resulted in the changes in the UV-vis spectrum of Fc^+-containing **5–7** in comparison with Fc-tethered stating materials **2–4**, which is in a good agreement with the absorption spectral studies on the oxidation of simple Fc and Fc^+ containing systems (see UV-Vis spectra of **5–7** in ESI, Subsection S4.1†).[48,53,61,62] The UV-vis analyses in acetone–water solvent mixtures revealed that among the tested Fc^+-containing sumanene derivatives **5–7**, the water solubility of compound **7** (tetracation) is the most satisfactory (see spectra and discussion in ESI, Subsection S4.2†).

Application of compounds 5–7 as anticancer agents

Full details on biological assays can be found in ESI, Subsection S1† (key-procedure details are also listed below in the Experimental section).

We anticipated that due to the presence of Fc^+ units in molecules **5–7**, these compounds might feature attractive cytotoxicity against cancer cells. Considering that the most common cancer worldwide is breast cancer,[38,39] cytotoxicity profiles were estimated *in vitro* against human breast adenocarcinoma cells (MDA-MB-231) as the representative breast cancer cell line, together with the respective studies with human mammary fibroblasts (HMF) as normal cells. The results of biological assays with Fc^+-containing **5–7** are presented in Fig. 5. The cytotoxicity profiles of native sumanene (**1**), Fc, $FcPF_6$, as well as patent Fc-containing mono-, tris- and tetra-ferrocenylated sumanene derivatives **2–4** are also presented for the reference. The biological assays were performed for three concentrations, namely 10, 50 and 100 μM. In general, for all tested compounds lower cell viabilities (after 24 hours) were observed for higher concentrations (50 and 100 μM). In the used model, the most essential differences in cell viabilities between the tested compounds were found for the lowest concentration, *i.e.*, 10 μM; thus, cell viabilities for this concentration were selected for most of the discussion on differences in the cytotoxicity profiles of the tested compounds.

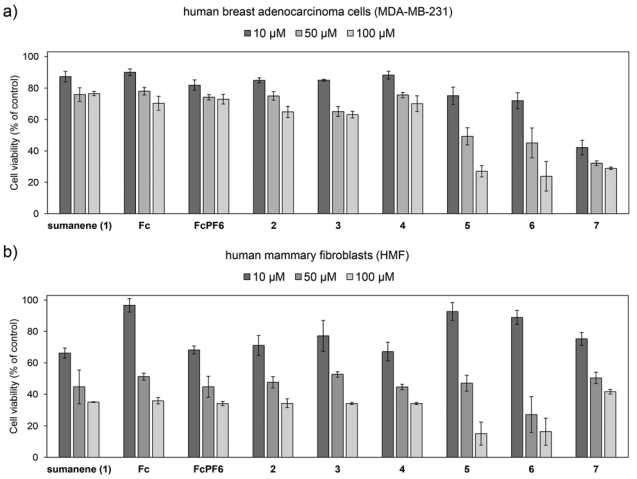

Fig. 5 Cell viabilities (after 24 hours) after treatment with sumanene (**1**), Fc, $FcPF_6$ and compounds **2–7**: (a) MDA-MB-231 (breast cancer) cells and (b) human mammary fibroblasts (HMF, normal cells).

In the used model, native Fc featured a slight cytotoxic effect towards MDA-MB-231 cancer cells (cell viability: *ca.* 94% for 10 μM), whilst the cell viability of HMF normal cells was similar to that of the control (*ca.* 97% for 10 μM). $FcPF_6$ featured improved cytotoxicity against MDA-MB-231 cancer cells (cell viability: *ca.* 75% for 10 μM) in comparison with Fc. HMF normal cell viability after the treatment with $FcPF_6$ equalled *ca.* 68% for 10 μM. Sumanene (**1**) featured slightly lower cytotoxicity against MDA-MB-231 cancer cells (cell viability *ca.* 84% for 10 μM) in comparison with $FcPF_6$, whilst cytotoxicity against HMF normal cells was similar to that of $FcPF_6$. It means that $FcPF_6$ featured better cancer-specific cytotoxic action than sumanene (**1**). In the case of ferrocene-containing sumanene derivatives **2–4**, cell viabilities of MDA-MB-231 cancer cells were at the level of *ca.* 82–85% for 10 μM, which means that these molecules featured cytotoxicity profiles similar to sumanene (**1**) and improved cytotoxicity in comparison with native Fc. The cell viability of HMF normal cells after the treatment with **2–4** ranged from *ca.* 67 to *ca.* 77% for 10 μM.

Significant differences between the cytotoxicity profiles of Fc^+-containing sumanene derivatives **5–7** *versus* Fc, sumanene (**1**) and parent Fc derivatives **2–4** were observed. The cytotoxicity profiles of compounds **5–7** towards MD-MB-231 cells were improved in comparison with those of not only the parent compounds **2–4**, but also native sumanene (**1**). This suggested that the presence of Fc^+ units attached to the sumanene skeleton resulted in the improved anticancer potential of these molecules, associated with the oxidation state of iron.

Open Access Article. Published on 30 November 2023. Downloaded on 2/9/2026 12:15:48 PM.
This article is licensed under a Creative Commons Attribution 3.0 Unported Licence.

Compounds **5–7** featured higher cytotoxicity towards MDA-MB-231 cancer cells (*ca.* 23–70%) than other tested compounds, also including $FcPF_6$. This was especially observed for higher concentrations (*ca.* 32–49% for 50 μM and *ca.* 23–26% for 100 μM). Additionally, the satisfactory cancer-cell specific cytotoxic action of **5–7** was observed for the concentration of 10 μM, since at this concentration the viabilities of HMF normal cells were *ca.* 1.3–1.8-fold higher in comparison with the viability of MDA-MB-231 cancer cells.

Notably, the cytotoxicity profile for the Fc^+-containing sumanene derivative **7** was the most promising among all compounds tested. For the 10 μM concentration of compounds **5** and **6**, MDA-MB-231 cancer cell viability equaled *ca.* 72–77% and HMF normal cell viabilities were satisfactory (*ca.* 88%); however, compounds **5** and **6** were found to be relatively toxic for both cells at higher concentrations (50–100 μM). Compound **7** featured a significant cytotoxic effect towards MDA-MB-231 cancer cells for all tested concentrations (cell viability < 42%). Importantly, for the most beneficial concentration of 10 μM, MDA-MB-231 cancer cell viability after the treatment with **7** was *ca.* 40% and HMF normal cell viability (*ca.* 75%) was higher than those for $FcPF_6$, sumanene (**1**) and parent compound **4**. It can be concluded that compound **7** featured significant cytotoxicity against cancer cells due to the presence of sumanene and Fc^+ moieties. The Fc^+ motif also provided the selectivity of the anticancer action of the compound **7**. The biological properties of **7** were also improved in comparison with that of native building blocks, which suggested the effects of the presence of the sumanene skeleton on the anticancer action of this molecule. Similar beneficial cytotoxicity profiles of **7** could be also observed for higher concentrations. In other words, for the respective concentrations of compound **7**, the viability of HMF normal cells was 1.4–1.7-fold higher in comparison with that of MDA-MB-231 cancer cells. In consequence, compound **7** not only featured the best cytotoxicity against cancer cells among all compounds tested, but also the best selectivity of cytotoxic action. Taking into account the above-noted improved cancer-specific action of $FcPF_6$ in comparison with that of native sumanene (**1**), one might state that these beneficial cytotoxicity profiles of the sumanene buckybowl derivative **7** might be related to the presence of the highest number of ferrocenium residues in this molecule in comparison with compounds **5** and **6**, providing the most satisfactory cancer-specific features among the ferrocenium-tethered sumanene derivatives tested.

The level of ROS with the tested Fc^+-containing sumanene derivatives **5–7** was evaluated for MDA-MB-231 (breast cancer) cells to investigate the potential of these derivatives towards the generation of ROS. The results of this assay are presented in Fig. 6. In the used model, compounds **5–7** featured the property of generating ROS, elucidated by the higher level of ROS in comparison with the control for most tested concentrations. This suggested that the cytotoxic action of **5–7** was associated with the generation of ROS leading to the formation of radical metabolites responsible for biological damage to the cancer cells. The ROS levels of **5–7** were also higher in comparison with that of $FcPF_6$, as graphically presented in Fig. 6. The most satisfactory ROS level for all compounds was observed for the concentration of 10 μM. Notably, while compounds **5** and **6** were able to generate ROS only at this concentration, compound **7** was not only able to effectively generate ROS at all tested concentrations (10, 50 and 100 μM), but also the ROS levels of this derivative were the highest among the compounds tested. This further supported the most satisfactory biological action of compound **7** among the investigated Fc^+-containing sumanene derivatives concluded from *in vitro* assays with MDA-MB-231 cells (Fig. 6).

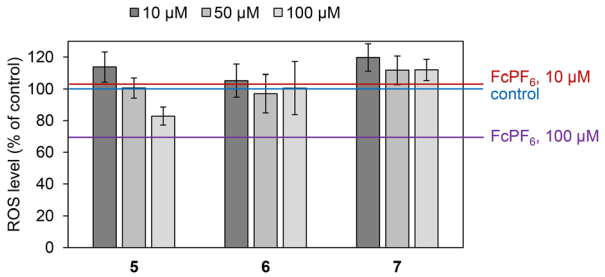

Fig. 6 Influence of compounds **5–7** on ROS generation in MDA-MB-231 (breast cancer) cells.

To finally elucidate the biological potential of **7**, as the most promising anticancer agent among the sumanene–ferrocenium conjugates tested, we intended to evaluate its embryotoxicity. The use of zebrafish embryos is one of the most attractive, leading toxicology models in this field, and it constitutes a suitable alternative for the use of small laboratory animals, such as rats or mice, due to short analysis times, short life cycle and transparency of embryos, and, importantly, zebrafish share approximately seventy percent protein-coding genes with humans.[63–65] Thus, zebrafish (*Danio rerio*) teratogenicity assays are commonly used for the prediction of the embryotoxic effects of chemicals, including new drug candidates. The images of zebrafish (*Danio rerio*) embryos treated with and without the compound **7** are presented in Fig. 7. To our delight, there was no observed mortality, change in hatching, or morphological alteration between zebrafish embryos

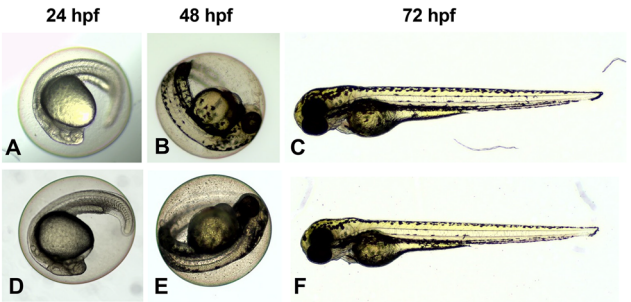

Fig. 7 Zebrafish embryos treated with (D–F) and without (A–C) compound **7** for 24 hpf (A and D), 48 hpf (B and E) and 72 hpf (C and F). (A–C) – Control (E3 with 0.1% DMSO) and (D–F) – compound **7** (50 μg mL^{-1}) with 0.1% DMSO (hpf – hours post-fertilization).

This journal is © The Royal Society of Chemistry 2024

Open Access Article. Published on 30 November 2023. Downloaded on 2/9/2026 12:15:48 PM. This article is licensed under a Creative Commons Attribution 3.0 Unported Licence.

exposed to compound 7 for all concentrations (1–50 μg mL^{-1}) tested and control embryos (E3 with 0.1% DMSO). We did not also observe any sublethal morphological malformations such as yolk or heart oedema, abnormal body shape, reduced yolk, impaired fin development, or eye malformation in all examined groups (Fig. 7). It means that the compound 7 showed no toxicity at the tested concentrations in zebrafish embryos.

Taking into account the growing importance of *in silico* modeling methods[66,67] on novel drug candidates related to the reduction of the usage of animal models before human trials,[68,69] ADME–Tox properties for compounds **4–7** were also assessed and the details are presented in ESI, Section S7.† In brief, *in silico* computational analysis showed no chromosomal aberrations and no mutation with AMES tests for the compound 7 tested with and without microsomal rat liver fractions, which supports its further use as a potent drug candidate in detailed anticancer studies.

Conclusions

In conclusion, the efficient and easy-to-perform method for the oxidation of ferrocene units in ferrocene–sumanene conjugates **2–4** into the derivatives **5–7** comprising ferrocenium cations (Fc^+) was achieved under mild conditions. Biological assays revealed that the target Fe^{III}-containing buckybowls represent an attractive class of anticancer agents towards killing breast cancer, as supported by *in vitro* cell viability assays with human breast adenocarcinoma cells. Among the compounds tested, the tetracationic sumanene derivative 7 featured the most satisfactory biological features. Compound 7 featured the best cytotoxic action towards cancer cells, with the cell viabilities of MDA-MB-231 cancer cells lower than 40% for all tested concentrations, together with the best selectivity towards killing cancer cells, with cell viabilities of HMF normal cells at the level of 75% (for the concentration of 10 μM). Reactive oxygen species (ROS) generation assay with MDA-MB-231 cancer cells revealed the potential of compounds **5–7** towards the generation of ROS responsible for biological damage to the cancer cells, with the most efficient effects for the tetra-ferrocenium sumanene derivative 7. Zebrafish (*Danio rerio*) teratogenicity assays with 7 also revealed no embryotoxic effects of this molecule, which is also *in silico*-predicted to have no clastogenic and mutagenic activities, supporting its potential as an anticancer drug candidate. Notably, while sumanene itself was found to be cytotoxic to cancer cells, it also featured significant cytotoxicity against normal cells. In fact, the attachment of ferrocenium residues to the sumanene backbone (compound 7 obtained) improved the biological action of native sumanene, in terms of cytotoxic action selective towards cancer cells. The cytotoxicity of ferrocenium hexafluorophosphate ($FcPF_6$) itself against cancer cells was also not as satisfactory as that of compound 7. Such conclusions thus revealed an effect of the presence of the sumanene backbone in 7 towards providing a good cytotoxicity profile of 7, also in terms of the improved selectivity of the cytotoxic action of 7 in comparison with that of $FcPF_6$. We believe that this work demonstrates the application potential of specifically designed sumanene derivatives in medicinal chemistry and opens new possibilities in this field of applied science of buckybowls.

Experimental section

Synthesis of 4

2-(Ferrocenylethynyl)sumanene (**2**; 21.6 mg, 0.046 mmol, 1 eq.) was placed in a reaction test tube. Tetrabutylammonium bromide (TBAB; 8.0 mg, 0.024 mmol, 0.5 eq.) was added, followed by the addition of dry THF (0.5 mL) and degassed $NaOH_{aq}$ (30%; 4 mL). The reaction mixture was stirred for 5 min at room temperature. Solid formylferrocene (**8**; 80.0 mg, 0.368 mmol, 8 eq.) was added in one portion, and the reaction mixture was stirred for 72 hours at room temperature. Distilled water (10 mL) was added, and the crude product was extracted with CH_2Cl_2 (3 × 25 mL). Organic layers were combined and washed with saturated NH_4Cl (10 mL), water (10 mL), and brine (10 mL). After drying with $MgSO_4$ followed by filtration, volatiles were distilled off on a rotary evaporator. Finally, the product was purified using a PTLC (SiO_2, 50% CH_2Cl_2/hexane) to provide the target compound **4** as a deep-red solid (34.1 mg, 70%).

^1H NMR (THF-d_8, 500 MHz, ppm), δ_H 8.22–8.19 (m, 1H), 8.05–8.02 (m, 0.5H), 7.89 (s, 0.5H), 7.76–7.64 (m, 2.5H), 7.47–7.46 (m, 0.5H), 7.37–7.26 (m, 3H), 5.27–5.08 (m, 3H), 4.83–4.48 (m, 12H), 4.40–4.22 (m, 21H); $^{13}C\{^1H\}$ NMR (THF-d_8, 125 MHz, ppm), δ_C 147.5, 147.3, 146.3, 146.2, 145.2, 145.0, 144.0, 142.2, 138.6, 138.4, 137.7, 131.6, 131.5, 131.3, 129.4, 129.2, 129.0, 128.8, 128.3, 126.1, 125.2, 125.1, 125.0, 124.8, 124.6, 124.5, 122.4, 121.7 × 2, 121.5, 121.3, 121.1, 93.4, 93.2, 82.0, 81.9, 81.8, 72.8, 72.7, 72.5, 72.3, 72.0, 71.7, 71.6, 71.4, 71.3, 71.1, 70.8, 70.6, 70.2; HRMS (ESI) m/z $[M]^+$ calcd for $C_{66}H_{44}Fe_4$ 1060.0835, found 1060.0840; R_f (50% CH_2Cl_2/hexane) = 0.37.

General procedure for the synthesis of 5–7

Compounds **2–4** (0.02 mmol, 1 eq.) were placed in a reaction flask. The content of the flask was evacuated and purged with argon. Dry DCM (5 mL) was added, and the content of the flask was cooled to −20 °C. A solution of silver(I) hexafluorophosphate ($AgPF_6$; 0.06 mmol, 4 eq.) in dry DCM (3 mL) was slowly added at −20 °C. The addition of $AgPF_6$ resulted in a color change, as well as the formation of a brownish precipitate. The reaction mixture was stirred for 10 min at room temperature, filtered off and washed with DCM and EtOH. Finally, after drying under high vacuum for several hours, compounds **5–7** were obtained.

Compound 7. Dark-brown solid, quantitative yield. ^1H NMR (DMSO-d_6, 500 MHz, ppm), δ_H 8.13–8.12 (m,1H), 7.99–7.98 (m, 0.5H), 7.74–7.60 (m, 3.5H), 7.54–7.53 (m, 0.5H), 7.50–7.45 (m, 2.5H), 5.18–4.88 (m, 3H), 4.78–4.47 (m, 12H), 4.37–4.25 (m, 21H); ^{19}F NMR (DMSO-d_6, 500 MHz, ppm, C_6F_6 was used as the internal standard), δ_F −72.46 ppm (d, J = 711.3 Hz, 24F).

Open Access Article. Published on 30 November 2023. Downloaded on 2/9/2026 12:15:48 PM.
This article is licensed under a Creative Commons Attribution 3.0 Unported Licence.

^{1}H NMR ($(CD_3)_2CO$, 500 MHz, ppm), δ_H 32.85 (bs), 29.85 (bs), 32.85 (bs), 27.28–26.62 (bm), 23.94 (bs), 19.5–18.2 (bm), 15.16 (bs); ^{19}F NMR ($(CD_3)_2CO$, 500 MHz, ppm, C_6F_6 was used as the internal standard), δ_F −77.70 ppm (d, J = 708.0 Hz, 24F). Due to the poor solubility of compound **7** no good quality $\{^1H\}^{13}C$ NMR spectrum could be obtained; therefore elemental analysis was additionally performed for this compound; elemental analysis: anal. calcd for $C_{66}H_{44}F_{24}Fe_4P_4$: C, 48.33; H, 2.70. Found: C, 48.09; H, 2.72; HRMS (ESI) m/z $[M]^+$ calcd for $C_{66}H_{44}F_{24}Fe_4P_4$ 1639.9402, found 1639.9409.

Compound 6. Dark-brown solid, quantitative yield. ^{1}H NMR (DMSO-d_6, 500 MHz, ppm), δ_H 7.71–7.66 (bm, 3H), 7.51–7.42 (bm, 6H), 5.09–5.06 (bm, 3H), 4.75–4.58 (bm, 9H), 4.33–4.30 (nm, 15H); ^{19}F NMR (DMSO-d_6, 500 MHz, ppm, C_6F_6 was used as the internal standard), δ_F −72.39 ppm (d, J = 711.3 Hz, 18F). ^{1}H NMR ($(CD_3)_2CO$, 500 MHz, ppm), δ_H 37.16–34.38 (bm), 30.06 (bs), 20.59–19.91 (bm); ^{19}F NMR ($(CD_3)_2CO$, 500 MHz, ppm, C_6F_6 was used as the internal standard), δ_F −72.96 ppm (d, J = 707.3 Hz, 18F). Due to the poor solubility of compound **6** no good quality $\{^1H\}^{13}C$ NMR spectrum could be obtained; therefore elemental analysis was additionally performed for this compound; elemental analysis: anal. calcd for $C_{54}H_{36}F_{18}Fe_3P_3$: C, 50.38; H, 2.82. Found: C, 50.08; H, 2.84; HRMS (ESI) m/z $[M]^+$ calcd for $C_{54}H_{36}F_{18}Fe_3P_3$ 1286.97852, found 1286.97860.

Compound 5. Dark-brown solid, quantitative yield. ^{1}H NMR ($(CD_3)_2CO$, 500 MHz, ppm), δ_H 29.94 (bs), 14.84 (bs); ^{19}F NMR ($(CD_3)_2CO$, 500 MHz, ppm, C_6F_6 was used as the internal standard), δ_F −73.82 ppm (d, J = 707.4 Hz, 6F). Due to the poor solubility of compound **5** no good quality $\{^1H\}^{13}C$ NMR spectrum could be obtained; therefore elemental analysis was additionally performed for this compound; elemental analysis: anal. calcd for $C_{33}H_{20}F_6Fe_1P_1$: C, 64.21; H, 3.27. Found: C, 63.82; H, 3.29; HRMS (ESI) m/z $[M]^+$ calcd for $C_{33}H_{20}F_6Fe_1P_1$ 617.05508, found 617.05512.

Biological tests

Cell culture. MDA-MB 231 cells were obtained from ATCC Europe Collection and were maintained in high glucose Dulbecco's modified Eagle's medium (DMEM, Biowest, L0102) with 10% fetal bovine serum (FBS, Biowest, S181B), 1% penicillin–streptomycin (Biowest, L0022) and 1% L-glutamine (Biowest, X0550). HMF cells were obtained from ScienCell (#7630) and were maintained in Fibroblast Medium (FM, #2301). All cell lines were cultured using standard protocols with Phosphatase Buffer Saline (PBS, Sigma-Aldrich, P54931L) and trypsin 0.25%–EDTA (Biowest, L0931).

Cell seeding and toxicology studies. 96-Well plates (Nest Scientific Biotechnology, 701001) were used for monolayer cell formation. The MDA-MB 231 or HMF cells were seeded with a density of 10^4 cells per well and incubated overnight (5% CO_2, 35 °C). After the medium was removed, all tested drugs/compounds in proper concentrations were added to the wells. The monolayer cultured with media was recognized as a negative control. After 24 h the cell metabolic activity evaluation with alamarBlue® assay (AB, Serotec Ltd, Oxford, UK) was performed. For this purpose, 10% AB solution, prepared in a cell culture medium, was added to each well and incubated for 1 h (5% CO_2, 37 °C). After this, the fluorescence intensity was measured using a plate reader (Cytation™3, BioTek) at the excitation and emission wavelength of 552 nm and 583 nm, respectively.

ROS. 24 h after drug treatment, the MDA-MB 231 cells were washed with PBS solution (Sigma Aldrich). Then, a 20 μM 2′,7′-dichlorofluorescein diacetate (DCFH-DA; Sigma Aldrich) solution prepared in culture medium without phenol red and bovine serum was added to the cells and incubated in the dark for 30 min (37 °C and 5% CO_2). After this time, the cells were washed with fresh PBS solution and the fluorescence intensity was measured at 485 nm and 530 nm for excitation and emission, respectively.

Embryotoxicity trials on compound 7 with zebrafish embryos. Zebrafish embryos (ABxTL) were obtained from the International Institute of Molecular and Cell Biology (IIMCB) in Warsaw and maintained in E3 medium. The embryos were identified according to Kimmel *et al.*,[70] and only the fertilized embryos showing the process of cell division were selected for studies. At 1.5 hours post-fertilization (hpf), the embryos were placed on 96-well plates with one embryo in 200 μL testing solution per well[71] with previously prepared solutions of the compound **7** dissolved in 0.1% DMSO with concentrations of 1 μg mL^{-1}, 10 μg mL^{-1}, 25 μg mL^{-1} and 50 μg mL^{-1}. We used 20 embryos for each concentration of the compound **7**, and the toxicity assessment was performed in three replicates. A total number of 300 embryos were used in this experiment. The plates were incubated at a constant temperature of 27 °C with a light–dark cycle (12 h/12 h) throughout the study period. Observations were made at 24-hour intervals up to 72 hpf. Mortality, hatching rate, and morphological changes were examined during observation. The lethality criteria were selected based on OECD TG 236 [72] including coagulation, lack of somite formation, no heartbeat, or non-detachment of the tail. The embryos were analyzed under an Olympus CKX53, and images were captured using an Olympus EP50 camera. A tricaine (0.3%) solution was applied at the end of the experiment for euthanasia.

Conflicts of interest

There are no conflicts to declare.

Acknowledgements

The financial support from the National Science Centre, Poland, OPUS grant no. 2021/43/B/ST4/00114 (A. K.), Warsaw University of Technology (WUT; A. K.), as well as JSPS KAKENHI (grant no. JP19H00912 and JP21H05233; H. S.) is acknowledged. The IIMCB Zebrafish Core Facility for service and fish material is also acknowledged.

 This journal is © The Royal Society of Chemistry 2024

Open Access Article. Published on 30 November 2023. Downloaded on 2/9/2026 12:15:48 PM. This article is licensed under a Creative Commons Attribution 3.0 Unported Licence.

References

1 H. Sakurai, T. Daiko and T. Hirao, *Science*, 2003, **301**, 1878.
2 M. Saito, H. Shinokubo and H. Sakurai, *Mater. Chem. Front.*, 2018, **2**, 635–661.
3 T. Amaya and T. Hirao, *Chem. Rec.*, 2015, **15**, 310–321.
4 T. Amaya and T. Hirao, *Chem. Commun.*, 2011, **47**, 10524.
5 S. Alvi and R. Ali, *Beilstein J. Org. Chem.*, 2020, **16**, 2212–2259.
6 H. Sakurai, T. Daiko, H. Sakane, T. Amaya and T. Hirao, *J. Am. Chem. Soc.*, 2005, **127**, 11580–11581.
7 S. N. Spisak, Z. Wei, A. Yu. Rogachev, T. Amaya, T. Hirao and M. A. Petrukhina, *Angew. Chem., Int. Ed.*, 2017, **56**, 2582–2587.
8 T. Amaya, W. Wang, H. Sakane, T. Moriuchi and T. Hirao, *Angew. Chem., Int. Ed.*, 2010, **49**, 403–406.
9 T. Amaya and T. Hirao, in *Advances in Organometallic Chemistry and Catalysis*, ed. A. J. L. Pombeiro, John Wiley & Sons, Inc., Hoboken, NJ, USA, 2013, pp. 473–483.
10 T. Amaya, H. Sakane and T. Hirao, *Angew. Chem.*, 2007, **119**, 8528–8531.
11 H. Sakane, T. Amaya, T. Moriuchi and T. Hirao, *Angew. Chem., Int. Ed.*, 2009, **48**, 1640–1643.
12 T. Amaya, Y. Takahashi, T. Moriuchi and T. Hirao, *J. Am. Chem. Soc.*, 2014, **136**, 12794–12798.
13 J. Han, Y. Yakiyama, Y. Takeda and H. Sakurai, *Inorg. Chem. Front.*, 2023, **10**, 211–217.
14 Y. Yakiyama, T. Hasegawa and H. Sakurai, *J. Am. Chem. Soc.*, 2019, **141**, 18099–18103.
15 A. Kasprzak and H. Sakurai, *Dalton Trans.*, 2019, **48**, 17147–17152.
16 A. Kasprzak, A. Kowalczyk, A. Jagielska, B. Wagner, A. M. Nowicka and H. Sakurai, *Dalton Trans.*, 2020, **49**, 9965–9971.
17 A. Kasprzak, A. Gajda-Walczak, A. Kowalczyk, B. Wagner, A. M. Nowicka, M. Nishimoto, M. Koszytkowska-Stawińska and H. Sakurai, *J. Org. Chem.*, 2023, **88**, 4199–4208.
18 J. S. Cyniak, Ł. Kocobolska, N. Bojdecka, A. Gajda-Walczak, A. Kowalczyk, B. Wagner, A. M. Nowicka, H. Sakurai and A. Kasprzak, *Dalton Trans.*, 2023, **52**, 3137–3147.
19 D. Astruc, *Eur. J. Inorg. Chem.*, 2017, 6–29.
20 F. A. Larik, A. Saeed, T. A. Fattah, U. Muqadar and P. A. Channar, *Appl. Organomet. Chem.*, 2017, **31**, e3664.
21 P. Štěpnička, *Dalton Trans.*, 2022, **51**, 8085–8102.
22 R. Wang, H. Chen, W. Yan, M. Zheng, T. Zhang and Y. Zhang, *Eur. J. Med. Chem.*, 2020, **190**, 112109.
23 C. Ornelas, *New J. Chem.*, 2011, **35**, 1973.
24 L. V. Snegur, *Inorganics*, 2022, **10**, 226.
25 M. Koszytkowska-Stawińska and W. Buchowicz, *Dalton Trans.*, 2023, **52**, 1501–1517.
26 P. Köpf-Maier, H. Kopf and E. W. Neuse, *J. Cancer Res. Clin. Oncol.*, 1984, **108**, 336–340.
27 D. Osella, M. Ferrali, P. Zanello, F. Laschi, M. Fontani, C. Nervi and G. Cavigiolio, *Inorg. Chim. Acta*, 2000, **306**, 42–48.
28 G. Tabbì, C. Cassino, G. Cavigiolio, D. Colangelo, A. Ghiglia, I. Viano and D. Osella, *J. Med. Chem.*, 2002, **45**, 5786–5796.
29 M. F. R. Fouda, M. M. Abd-Elzaher, R. A. Abdelsamaia and A. A. Labib, *Appl. Organomet. Chem.*, 2007, **21**, 613–625.
30 C. Y. A. Morantes, E. Meléndez, S. P. Singh and J. E. Ramírez-Vick, *J. Cancer Sci. Ther.*, 2012, **4**, 271–275.
31 Z. Chen, R. Mao and Y. Liu, *Curr. Drug Metab.*, 2012, **13**, 1035–1045.
32 L. Tang, Q. Xiao, Y. Mei, S. He, Z. Zhang, R. Wang and W. Wang, *J. Nanobiotechnol.*, 2021, **19**, 423.
33 J. Li, H. Zeng, Z. Zeng, Y. Zeng and T. Xie, *ACS Biomater. Sci. Eng.*, 2021, **7**, 5363–5396.
34 M. Mattarella, J. Garcia-Hartjes, T. Wennekes, H. Zuilhof and J. S. Siegel, *Org. Biomol. Chem.*, 2013, **11**, 4333–4339.
35 S. Liu, Z. Sun, M. Liang, W. Song, R. Zhang, Y. Shi, Y. Cui and Q. Gao, *Adv. Sci.*, 2022, **9**, 2105315.
36 J. S. Al-Otaibi, Y. S. Mary, Y. S. Mary, A. Mondal, N. Acharjee and D. G. Churchill, *Comput. Theor. Chem.*, 2022, **1215**, 113811.
37 (*a*) T. Reichert, M. Vučićević, P. Hillman, M. Bleicher, S. J. Armaković and S. Armaković, *J. Mol. Liq.*, 2021, **342**, 117526; (*b*) M. Nezamabadi, E. Balali and M. Qomi, *Inorg. Chem. Commun.*, 2023, **155**, 111098.
38 R. Hong and B. Xu, *Cancer Commun.*, 2022, **42**, 913–936.
39 N. Harbeck, F. Penault-Llorca, J. Cortes, M. Gnant, N. Houssami, P. Poortmans, K. Ruddy, J. Tsang and F. Cardoso, *Nat. Rev. Dis. Primers*, 2019, **5**, 66.
40 T. Amaya, K. Mori, H.-L. Wu, S. Ishida, J. Nakamura, K. Murata and T. Hirao, *Chem. Commun.*, 2007, 1902–1904.
41 A. Kasprzak, A. Tobolska, H. Sakurai and W. Wróblewski, *Dalton Trans.*, 2022, **51**, 468–472.
42 A. Kasprzak and H. Sakurai, *Chem. Commun.*, 2021, **57**, 343–346.
43 S. Fery-Forgues and B. Delavaux-Nicot, *J. Photochem. Photobiol., A*, 2000, **132**, 137–159.
44 J. Lehr, M. Tropiano, P. D. Beer, S. Faulkner and J. J. Davis, *Chem. Commun.*, 2015, **51**, 6515–6517.
45 E. Laviron, L. Roullier and C. Degrand, *J. Electroanal. Chem. Interfacial Electrochem.*, 1980, **112**, 11–23.
46 D. Vijay, H. Sakurai, V. Subramanian and G. N. Sastry, *Phys. Chem. Chem. Phys.*, 2012, **14**, 3057.
47 N. G. Connelly and W. E. Geiger, *Chem. Rev.*, 1996, **96**, 877–910.
48 A. J. Plajer, F. J. Rizzuto, L. K. S. Von Krbek, Y. Gisbert, V. Martínez-Agramunt and J. R. Nitschke, *Chem. Sci.*, 2020, **11**, 10399–10404.
49 Š. Toma and R. Šebesta, *Synthesis*, 2015, 1683–1695.
50 G. Noirbent, D. Brunel, T.-T. Bui, S. Péralta, P.-H. Aubert, D. Gigmes and F. Dumur, *New J. Chem.*, 2021, **45**, 13475–13498.
51 M. Nakahata, Y. Takashima, H. Yamaguchi and A. Harada, *Nat. Commun.*, 2011, **2**, 511.
52 G. Wilkinson, M. Rosenblum, M. C. Whiting and R. B. Woodward, *J. Am. Chem. Soc.*, 1952, **74**, 2125–2126.
53 D. A. Khobragade, S. G. Mahamulkar, L. Pospíšil, I. Císařová, L. Rulíšek and U. Jahn, *Chem. – Eur. J.*, 2012, **18**, 12267–12277.
54 H. B. Gray, D. N. Hendrickson and Y. S. Sohn, *Inorg. Chem.*, 1971, **10**, 1559–1563.

Open Access Article. Published on 30 November 2023. Downloaded on 2/9/2026 12:15:48 PM.
This article is licensed under a Creative Commons Attribution 3.0 Unported Licence.

55 A. Kasprzak, A. M. Nowicka, J. P. Sek, M. Fronczak, M. Bystrzejewski, M. Koszytkowska-Stawinska and M. Poplawska, *Dalton Trans.*, 2018, **47**, 30–34.
56 J. C. Smart and B. L. Pinsky, *J. Am. Chem. Soc.*, 1980, **102**, 1009–1015.
57 K. Venkatasubbaiah, I. Nowik, R. H. Herber and F. Jäkle, *Chem. Commun.*, 2007, 2154–2156.
58 Our initial attempts on oxidation of **2–4** in acetone using aqueous solution of iron(III) chloride, followed by the treatment with solid ammonium hexafluorophosphate were unsuccessful (NMR analyses only showed the regeneration of the starting materials, *ca*. 90%). We anticipated that this might be the result of the very poor solubility of sumanene–ferrocene conjugates **2–4** in acetone.
59 H. Song, G. Kwon, C. Citek, S. Jeon, K. Kang and E. Lee, *ACS Appl. Mater. Interfaces*, 2021, **13**, 46558–46565.
60 F. S. T. Khan, A. L. Waldbusser, M. C. Carrasco, H. Pourhadi and S. Hematian, *Dalton Trans.*, 2021, **50**, 7433–7455.
61 A. T. Liu, Y. Kunai, A. L. Cottrill, A. Kaplan, G. Zhang, H. Kim, R. S. Mollah, Y. L. Eatmon and M. S. Strano, *Nat. Commun.*, 2021, **12**, 3415.
62 H.-G. Xu, S. Annamadov and A. Mokhir, *J. Organomet. Chem.*, 2022, **964**, 122305.
63 A. Modarresi Chahardehi, H. Arsad and V. Lim, *Plants*, 2020, **9**, 1345.
64 J. C. Achenbach, C. Leggiadro, S. A. Sperker, C. Woodland and L. D. Ellis, *Toxics*, 2020, **8**, 126.
65 K. C. Brannen, J. M. Panzica-Kelly, T. L. Danberry and K. A. Augustine-Rauch, *Birth Defects Res., Part B*, 2010, **89**, 66–77.
66 A. V. Sadybekov and V. Katritch, *Nature*, 2023, **616**, 673–685.
67 S. Alqahtani, *Expert Opin. Drug Metab. Toxicol.*, 2017, **13**, 1147–1158.
68 M. Wadman, *Science*, 2023, **379**, 127–128.
69 S. K. Niazi, *Science*, 2022, **377**, 162–163.
70 C. B. Kimmel, W. W. Ballard, S. R. Kimmel, B. Ullmann and T. F. Schilling, *Dev. Dyn.*, 1995, **203**, 253–310.
71 S. Xu, F. Chen, H. Zhang, Z. Huang, J. Li, D. Wu and X. Chen, *Toxicol. Mech. Methods*, 2023, **33**, 104–112.
72 OECD, Fish Embryo Acute Toxicity (FET) Test, 2013, Test No. 236.

This journal is © The Royal Society of Chemistry 2024